

*Full Length Research Paper*

# Discrimination between oil spill and look-alike using fractal dimension algorithm from RADARSAT-1 SAR and AIRSAR/POLSAR data

Maged Marghany\* and Mazlan Hashim

Institute of Geospatial Science and Technology (INSTeG), Universiti Teknologi Malaysia 81310 UTM, Skudai, Johore Bahru, Malaysia.

Accepted 14 March, 2011

**This work utilizes a modification of the formula of the fractal box counting dimension in which a convoluted line of slick embedded in SAR data was divided into small boxes. The method is based on the utilization of the probability distribution formula in the fractal box count. The purpose of this method is to use it for the discrimination of oil spill areas from the surrounding features, for example, sea surface and look-alikes in SAR data, that is, RADARSAT-1 SAR S2 mode and AIRSAR/POLSAR data. The results show that the modified formula of the fractal box counting dimension can discriminate between oil spills and look-alike areas. The low wind area has the highest fractal dimension peak of 2.9, as compared to the oil slick and the surrounding rough sea. Further, modified formula of fractal box counting dimension is also able to detect look-alikes and low wind zone areas in AIRSAR/POLSAR data. It is interesting to find out that oil spill is absent in AIRSAR/POLSAR data. Both SAR data have a maximum error standard deviation of 0.45, which performs with fractal dimension value of 2.9. In conclusion, modification formula of fractal box counting dimension is a promising technique for oil spill and look-alikes automatic discrimination in different sensor of SAR data.**

**Key words:** Oil spill, look-alikes, fractal dimension, RADARSAT-1 SAR, AIRSAR/POLSAR.

## INTRODUCTION

Automatic detection of oil spill and look-alikes in synthetic aperture radar (SAR) is a required standard procedures. In fact, oil spill and look-alike appeared as dark patches in SAR data (Bern et al., 1993; Benelli and Garzelli, 1998; Teivero et al., 1998; Calaberesi et al., 1999; Aiazzi et al., 2000; Marghany et al., 2009a; Marghany and Mazlan, 2010a). Therefore, the most efficient technique used for oil spill and look-alikes discrimination is fractal box counting. According to Falconer (2003), fractals are a mathematical construct that describes a rough or fragmented geometric shape that is divided into similar partitions named as self-similarity. Furthermore, self-similarity, or statistical self-similarity, portraying exact self-similarity and quasi self-similarity are used to describe fractal. In this context, a fractal has consequent characteristics: (i) it has a simple and recursive definition,

(ii) self-similar, (iii) irregular to be easily described in traditional Euclidean geometric language, (iv) it has a Hausdorff dimension which is greater than its topological dimension (although this requirement is not met by space-filling curves such as the Hilbert curve), and (v) fine structure at an arbitrarily small scale (Tricot, 1993). Consequently, escape-time fractals, iterated function systems, strange attractors, and random fractals, are the major techniques to generate fractals. Fukunaga (1990), Milan et al. (1993) and Redondo (1996) agreed that exact self-similarity is the strongest fractal type than quasi-self-similarity and statistical self-similarity. Indeed, quasi-self-similar fractals contain small copies of the entire fractal in distorted and degenerate forms and statistical self-similarity has statistical measures which are preserved across scales. Thus, fractal dimension itself is a numerical measure which is preserved across scales (Pentland 1984; Briggs 1992; Falconer, 2003). Under this circumstance, fractal dimension is a statistical quantity which proposed of how extremely a fractal

\*Corresponding author. E-mail: [magedupm@hotmail.com](mailto:magedupm@hotmail.com).

occurs to fill space, as one zooms down to finer and finer scales. According to Falconer (2003), the Rényi dimension, the Hausdorff dimension and packing dimension are most tremendous theoretical fractal dimensions (Wornell and Oppenheim, 1992). Thus, the box-counting dimension and correlation dimension practically are widely used, partially because of their ease of implementation. Although for some classical fractals all these dimensions do coincide, in general they are not equivalent (Fukunaga, 1990; Falconer, 1990; Milan et al., 1993; Redondo, 1996).

The most well known procedures that have been proposed for estimating the fractal dimension of SAR images are box counting, fractal Brownian motion (Falconer, 1990; Gado and Redondo, 1999; Benelli and Garzelli, 1999) and fractal interpolation function system dimension of images (Aiuzzi et al., 2001). Initially, Falconer (1990) introduced the fractional Brownian motion model with SAR image intensity variation, which promises in the SAR data textures. In fact, both the sea surface and its backscattered signal in the SAR data can be modeled as fractals (Wornell and Oppenheim, 1992; Maragos and Sun, 1993; Benelli and Garzelli, 1999; Aiuzzi et al., 2001). Recently, Marghany et al. (2007, 2009a, b) have introduced a new formula of fractal box counting dimension. They modified the main fractal equation using probability distribution function formula. Marghany et al. (2009b) found out that the new fractal formula identifies properly the deficiency of oil spills in pairs of RADARSAT-1 SAR S2 mode data. Nevertheless, the new formula increased the fractal values in the area of ships, which differed from previous work of Garzelli (1999) and Aiuzzi et al. (2001).

By contrast, Gado and Redondo (1999) found that a box counting fractal dimension model provided excellent discrimination between oil spills and look-alikes, although the backscatter information, which could allow a first robust localization of the oil spills, had not been considered. Furthermore, Benelli and Garzelli (1999) used a multi-resolution algorithm which was based on fractal geometry for texture analysis. They found that the sea surface is characterized by an approximately steady value of fractal dimension, while the oil spills have a different average fractal dimension compared to look-alikes.

This study has theorized that the dark patches (oil slick or look-alike pixels) and their surrounding backscattered environmental signals in the SAR data can be modeled as fractals. In this context, a box-counting fractal estimator can be used as a semiautomatic tool to be discriminate between oil spills, look-alikes and surrounding sea surface waters. In addition, the utilization of a probability density formula in the box-counting equation can improve the accuracy of discrimination between oil slick pixels and surrounding feature pixels such as ocean surface and look-alikes. This study is the extension of previous studies of Marghany et al. (2007,

2009a, b) where airborne AIRSAR and POLSAR data used to validate the accuracy of modified fractal formula for discrimination between oil slicks and look-alikes.

## METHODOLOGY

### Data set

SAR data acquired in this study were derived from the RADARSAT-1 and AIRSAR/POLSAR images. RADARSAT-1 SAR data that involve standard beam mode (S2) images. S2 data are C-band and have a lower signal-to noise ratio due to their HH polarization with a wavelength of 5.6 cm and a frequency of 5.3 GHz. Further, S2 data have 3.1 looks and cover an incidence angle of 23.7° and 31.0° (Farahiday et al., 1998; Marghany and Mazlan, 2010a). In addition, S2 data cover a swath width of 100 km. Both Mohamed et al. (1999) and Marghany et al. (2009a) reported the occurrence of oil spill pollution on 20 December 1999, along the coastal water of the Malacca Straits.

The Jet Propulsion Laboratory (JPL) airborne, Airborne Synthetic Aperture Radar (AIRSAR) data. AIRSAR is a NASA/JPL multi-frequency instrument package aboard a DC-8 aircraft and operated by NASA's Ames Research Center at Moffett Field. AIRSAR flies at 8 km over the average terrain height at a velocity of 215 ms<sup>-1</sup>. The system is designed to be flown on small and large aircraft. The system requires a scanner port (18 cm x 36 cm) on the aircraft underside. JPL's airborne synthetic aperture radar (AIRSAR) is a unique system, comprising three radars at HH-, VV-, HV- and VH-polarized signals from 5 m x 5 m pixels recorded for three wavelengths: C band (5 cm), L band (24 cm) and P band (68 cm) (Zebker, 1992). AIRSAR data collections are involved; fully polarimetric data (POLSAR) can be collected at all three frequencies, while cross-track interferometric data (TOPSAR) and along-track interferometric (ATI) data can be collected at C- and L-bands (Marghany et al., 2010b; Marghany and Hashim, 2010c).

### Fractal algorithm for the oil spill identification

The oil slick detection tool uses fractal algorithms to detect the self-similar characteristics of RADARSAT-1 SAR and AIRSAR/POLSAR data intensity variations. A box-counting algorithm introduced by Benelli and Garzelli (1999) was used in this study. The box counting algorithm was used to divide a convoluted line of slick which was embedded in both SAR data plane (*i,j*), into smaller boxes. This was done by dividing the initial length of the convoluted line of the slick at backscatter level  $\beta_s$  by the recurrence level of the iteration (Gado and Redondo, 1999). Marghany et al. (2009a, b) defined a decreasing sequence of backscattering  $\beta_s$  tending from, the largest value, to less than or equal to zero. Following, Gado and Redondo (1999), the fractal dimension  $D(\beta_s)$  as a function of the

RADARSAT-1 SAR image intensity  $\beta_s$  is given by:

$$D(\beta_s) = D_B = \lim_{s \rightarrow \infty} \frac{\log M(\beta_s)}{-\log(\beta_s)} \quad (1)$$

where,  $M(\beta_s)$  denotes the number of boxes which are needed to cover the various slick areas with different backscatter intensity  $\beta_s$  in both SAR data. In addition, the subscript *s* indicates

the backscatter amplitude and its unit is  $dB$ . In practice, it is difficult to compute  $D(\beta_s)$  using Equation (1) due to the discrete RADARSAT-1 SAR and AIRSAR/POLSAR data surfaces, and so approximations to this relationship are employed. First, the RADARSAT-1 SAR and AIRSAR/POLSAR intensity images  $\beta$  is treated as a two-dimensional matrix ( $\beta \times \beta$ ). This  $\beta \times \beta$  intensity image matrix has been divided into non-overlapping or abutted windows of size  $l \times l$ , where  $l$  is the length of the convoluted line of the slick in both SAR data ( $\beta \times \beta$ ). In addition for each window, there is a column of accumulated boxes, each box with size of  $l_s^2 \times l$ . The backscatter values ( $\beta_0$ ) are stored at each intersection of the column  $i$  and row  $j$  of the various slick areas. Then  $l$  is calculated by using the differential box counting proposed by Sarkar and Chaudhuri (1994).

$$\left[ \frac{\beta_s}{l} \right] = \left[ \frac{\beta}{l_s} \right] \quad (2)$$

The number of boxes was non-overlapping which was calculated from the fractal dimension algorithm and having a square shape with side length  $l_s$  unit. This  $l_s$  is an odd, positive integer centred on an arbitrary point in the RADARSAT-1 SAR and AIRSAR/POLSAR backscatter images  $\beta_s$  surface. Therefore, side length was needed to cover a fractal profile, of backscatter image  $\beta_s^{-D}$ , where  $D$  is the fractal dimension that is to be estimated. Moreover, the box numbers were chosen based on the length of convoluted line of slick at backscatter level  $\beta_s$ . If the profile being sampled is a fractal object, then  $M(\beta_s)$  should be proportional to  $\beta_s^{-D}$  (Milan et al., 1993).

Let  $P[M(\beta_s), l_s]$  be the probability of the total number of boxes  $M(\beta_s)$  with box sizes  $l_s$ . This probability should be directly proportional to the number of boxes  $\sum_{i,j} n(\beta_0) - m(\beta_s) + 1$  spanned on the  $(i, j)$  windows. According to Marghany et al. (2009a, b) the expected number of boxes with size  $l_s$  which is needed to cover the slick pixels can be calculated using the following formula:

$$M(\beta_s) = \sum_{i,j} \frac{1}{n} P[M(\beta_s), l_s] \quad (3)$$

According to Fiscella et al. (2000), the probability distribution of the dark area belonging to slick pixels can be calculated using the formula below:

$$P[M(\beta_s)] = [1 + \prod_n q_n(M(\beta_s)) / p_n(M(\beta_s))] \quad (4)$$

Let  $n = \sum_{i,j} n(\beta_0) - m(\beta_s) + 1$ ,  $q$  and  $p$  are the probability distribution functions for look-alike and oil spill pixel areas, respectively. From Equations (3), (4) and (1) one can get a new formula for estimating the fractal dimension  $D_B$

$$D(\beta_s) = D_B = \lim_{s \rightarrow \infty} \frac{\log \sum_{i,j} n^{-1} [1 + \prod_n q_n(M(\beta_s)) / p_n(M(\beta_s))]}{-\log(\beta_s)} \quad (5)$$

According to Marghany et al. (2009a), Equation 5 represents the modification formula of Equation 1. In practice, the limit of  $M$  going to zero cannot be taken as it does not produce a texture image for oil spills or look-alikes in SAR data. Following Marghany et al. (2007), we may divide the slick's pixel areas into overlapping sub-images, using fractal dimensions to quantize texture for segmentation. Each sub-image is centred on the pixel of interest.

We then estimate the fractal dimension  $D(\beta_s)$  within each sub-image, and assign the fractal dimension value to the central pixel of each sub-image. This will produce a texture image that may be used as an additional feature in slick pixel classification.

## RESULTS AND DISCUSSION

The new fractal formula proposed by Marghany et al. (2009a, b) was trained on three SAR data, whereas the dark spots were identified and examined. The RADARSAT-1 SAR S2 mode image contained the confirmed oil spills that occurred 20 December 1999 (Samad and Shattri, 2002; Marghany, 2004; Marghany et al., 2009a) (Figure 1a). S2 mode data covered an area located in between  $101^\circ 01' 01.01''$  E to  $101^\circ 17' 11.5''$  E and  $2^\circ 25' 38.6''$  N to  $2^\circ 34' 23.5''$  N. The validation of new fractal formula was examined on pairs of AIRSAR/POLSAR data, which were acquired on 3 December 1996 from the coastline of Kuala Terengganu, Malaysia between  $103^\circ 5' E$  to  $103^\circ 9' E$  and  $5^\circ 20' N$  to  $5^\circ 27' N$ . The POLSAR data was acquired on 19 September 2000 from  $5^\circ 11' N$  to  $5^\circ 12' N$  and  $103^\circ 12' E$  to  $103^\circ 13' E$  along the southern of Kuala Terengganu, Merang port (Figures 1b and 1c) (Marghany et al., 2009b).

Figure 2 shows the variation of the average backscatter intensity along the azimuth direction in the oil-covered areas as a function of incidence angles for the S2 modes. The backscattered intensity was damped -10 dB to -18 dB in S2 (Figure 2). However, both AIRSAR/POLSAR data had higher backscatter intensities as compared to S2 mode data (Figure 2). Further, S2 and AIRSAR/POLSAR data backscatter intensities were well above noise floor value of nominally -20 dB. Indeed, RADARSAT-1 SAR is a C-band instrument with a variable acquisition swath, presenting a large variety of possible incidence angles, swath widths, and resolutions (Marghany et al., 2009a; Marghany and Mazlan, 2010a). Oil slicks can be detected with a contrast as small as 4

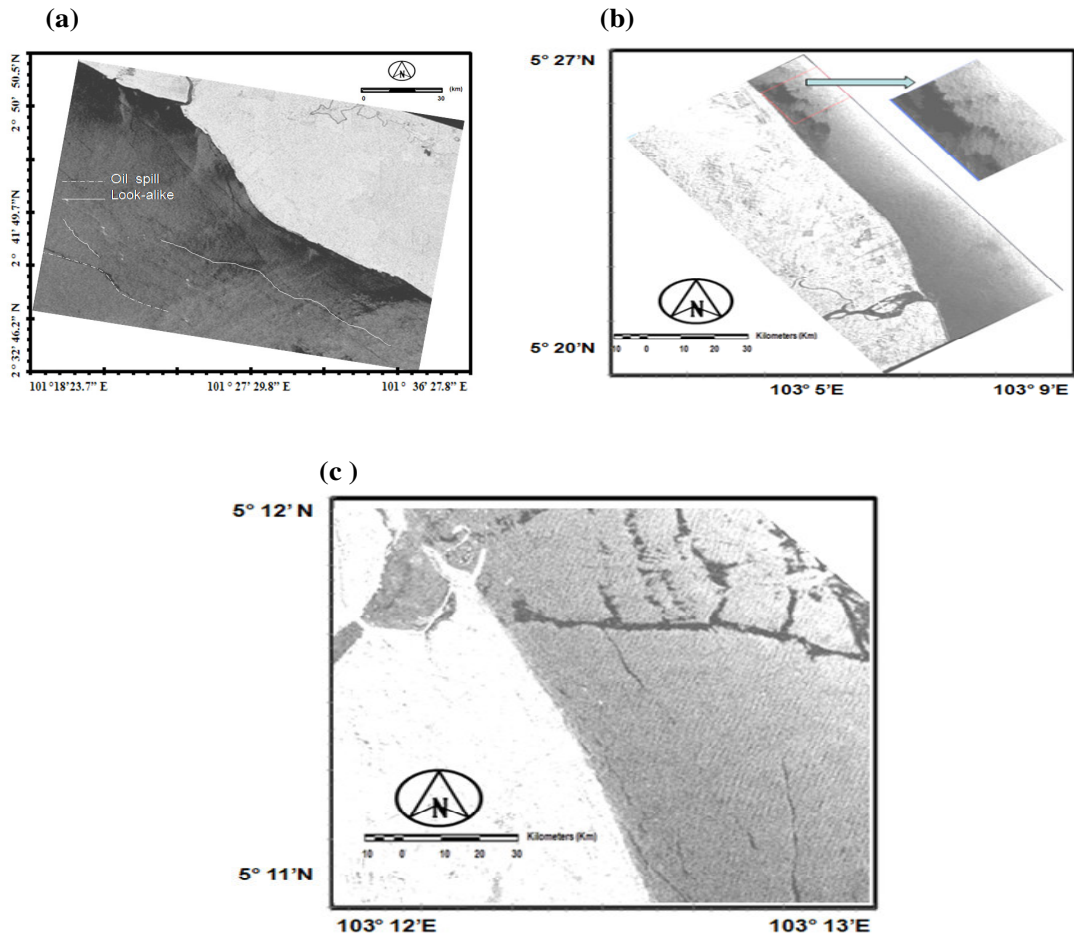


Figure 1. Oil spill in (a) RADARSAT-1 SAR S2 mode data and look-alikes at (b) AIRSAR data and (c) POLSAR data.

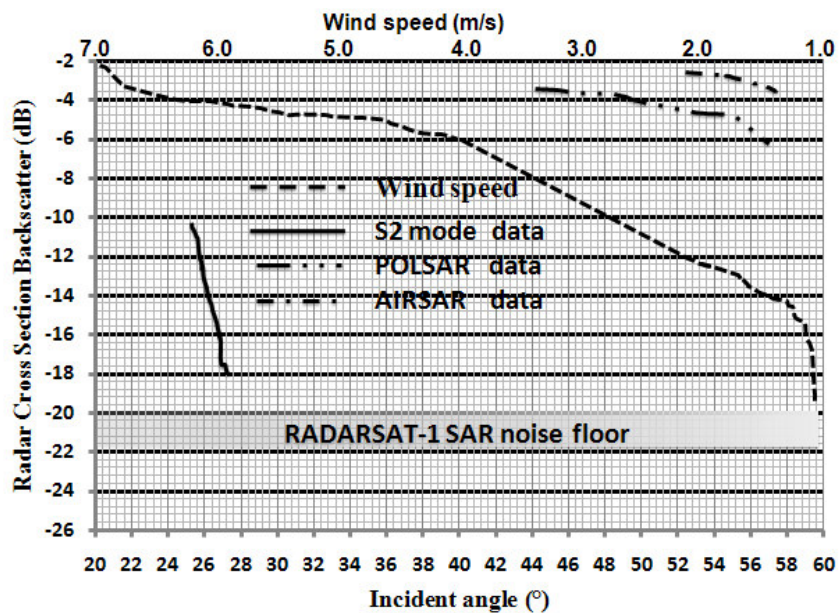
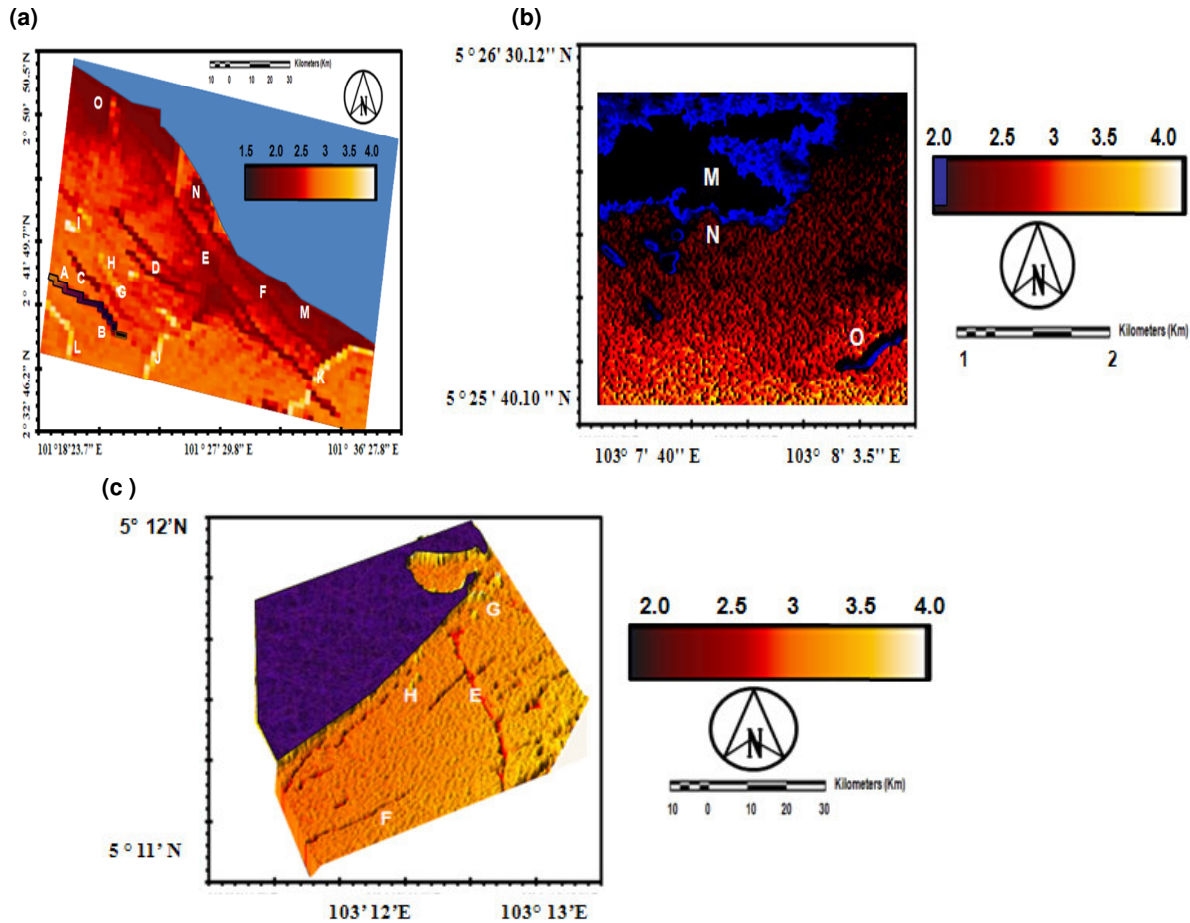


Figure 2. Radar cross section intensity along dark spots in SAR data.



**Figure 3.** Fractal map for (a) RADARSAT-1 SAR S2 mode data and (b) AIRSAR and (c) POLSAR.

dB (Kotova et al., 1998; Farahiday et al., 1998; Lu et al., 2000). This suggests that a large part of the RADARSAT-1 swath could be useful for oil slick detection. Nevertheless, Ivanov et al. (2002) reported that the RADARSAT-1 SAR, in its ScanSAR Narrow mode with swath width above 300 kms, was attractive for marine oil pollution detection.

The wind speed conditions acquired from the Malaysian Meteorological Survey Department showed a maximum offshore wind velocity of 4 m/s during the AIRSAR/POLSAR data overpass and 6.4 m/s and the acquisition of S2 mode data, respectively (Figure 2). In addition, the oil spill in the S2 mode with shallower incidence angle was between 23° and 27° (Figure 2), whereas in the AIRSAR/POLSAR data the dark spots were imaged by steeper incidence angles between 40° and 60° (Figure 2). According to Marghany and Mazlan (2005), steeper incidence angles are preferred for oil spill detection, since they tend to maximize the signal from the ocean surface. Our results of backscatter variations across oil spill locations agreed with the study of Marghany and Mazlan (2005).

The proposed method to estimate the fractal dimension was applied to the amplitude multi SAR data, by using a 10 x 10 block (Figure 3). The fractal dimension maps showed a good discrimination between different textures on the RADARSAT-1 SAR image and correlated well with image texture regions. This could be clearly noticed at area (H) where the ship and wake were well identified (Figure 3). The oil spill pixels were dominated by lower fractal values than look-alikes and surrounding environment (Figure 3a). In Figure 3a, the fractal values of oil spill regions varied between 1.49 and 2. According to Marghany et al. (2009a), the oil spill becomes thinner when the fractal dimension value increases. This could be noticed in areas A to C. In AIRSAR/POLSAR, however, oil spill is absent (Figures 3b and 3c). Indeed, a thick oil spill dampens the small-scale waves and therefore there is no Bragg resonance, which reduces the roughness of sea surface as compared to a thin oil spill (Bern et al., 1993). In this context, the fractal dimension is a function of sea surface level intensities over multi SAR data, which express the self-similarity (Benelli and Garzelli, 1999). In AIRSAR/POLSAR and S2 mode data,

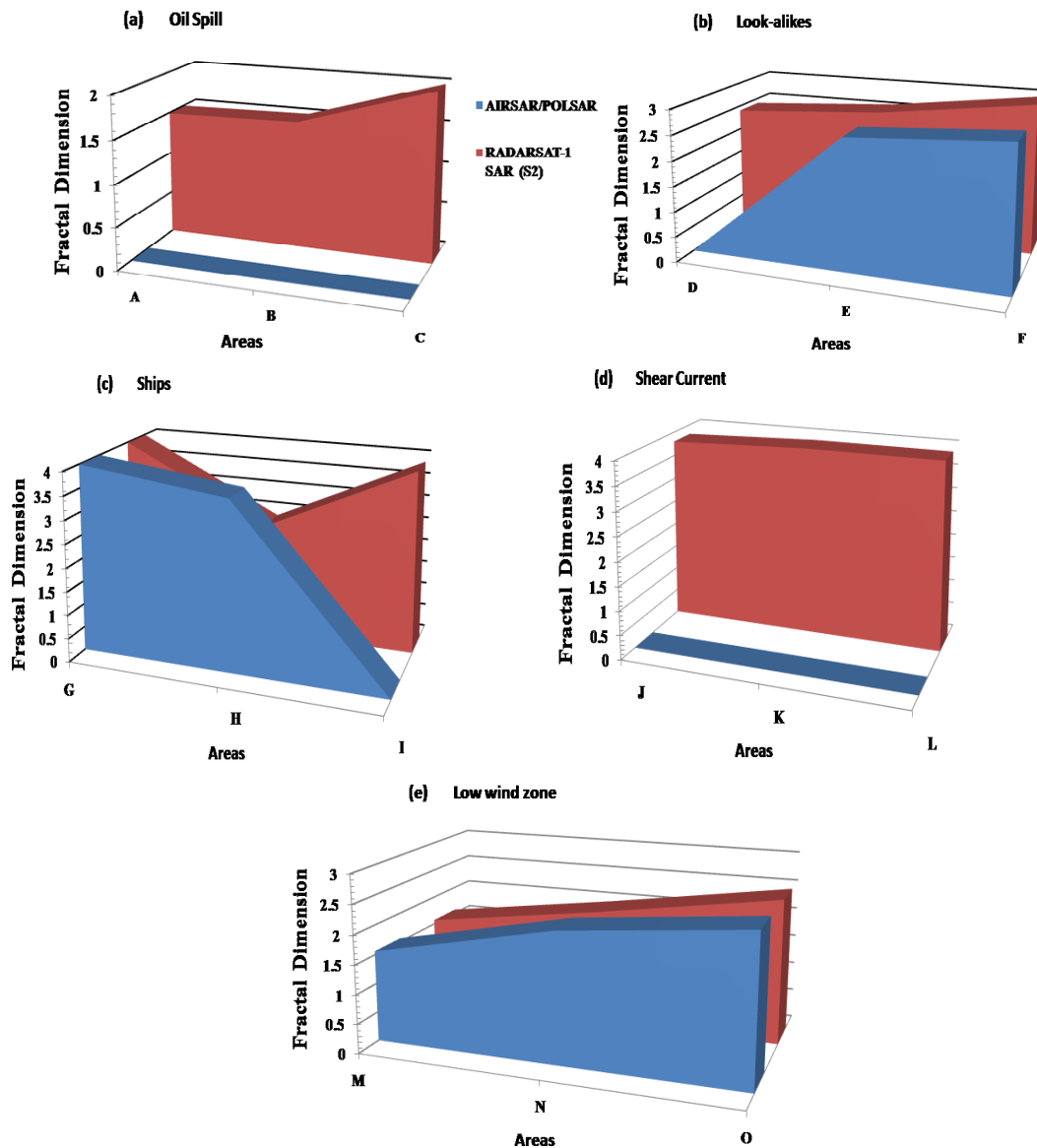


**Figure 4.** Fractal values for different features in RADARSAT-1 Standard (S2) mode and POLSAR/AIRSAR data (a) Oil spill, (b) Look-alikes, (c) ships, (d) shear current, and (e) low wind zone.

it could further be seen that low wind zones in areas M, N and O occurred close to the coastline, with maximum fractal values equal to 2.33, 2.34 and 2.5, respectively (Figure 3). Look-alikes occupied narrow areas parallel to the coastline (Figure 6). The wide distribution of dark zone pixels represented the natural slick in low wind areas (Henschel et al., 1997), which was aligned with what could be a current shear or convergence zone. This could be seen clearly in S1 mode data (Figure 3a). Thus, the fractal algorithm was able to discriminate the look-alike features from the surrounding sea surface features such as current shear (Figure 3a). Figure 3b illustrates, however, larger areas of look-alikes as compared to Figure 3a. The fractal dimension values of look-alikes

and ships are shown in Figures 3a, 3b and 3c were approximately similar.

In contrast to the S2 mode data, the fractal dimension values of look-alikes in AIRSAR/POLSAR data were higher (Figure 4a). In the AIRSAR/POLSAR, areas F and E represented the occurrence of look-alikes. Figure 4e shows that areas E and F (Figure 4b) in the POLSAR data corresponded to fractal dimension values 2.6 and 2.8, respectively, whereas area E corresponded to a fractal dimension equal to 2.6 in S2 mode data (4e). Figure 4c shows the highest fractal dimension values of 3.9 and 4.0 in areas I and G, respectively, were represented by the presence of a ship, whereas ship waves had a lower fractal dimension values, between 2.4

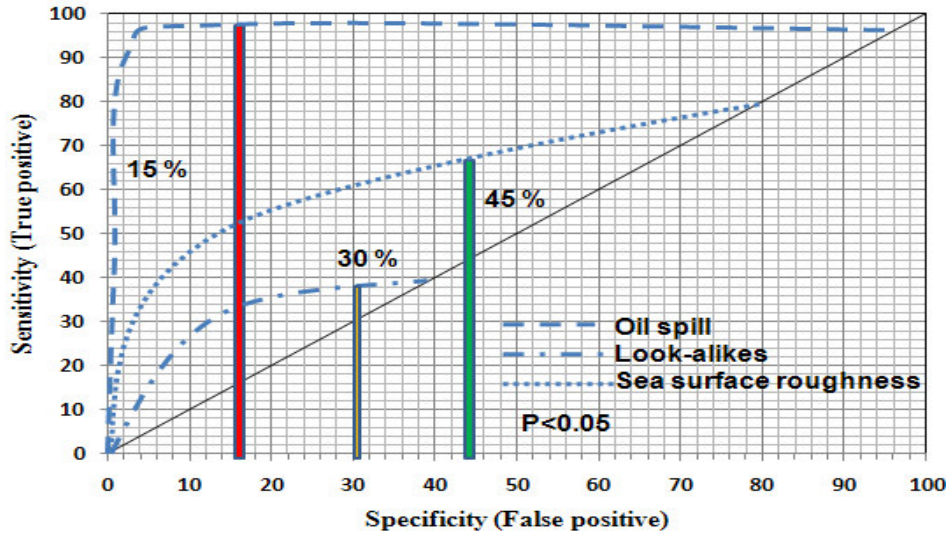


Figure 5. ROC Curve for different feature detection in SAR data.

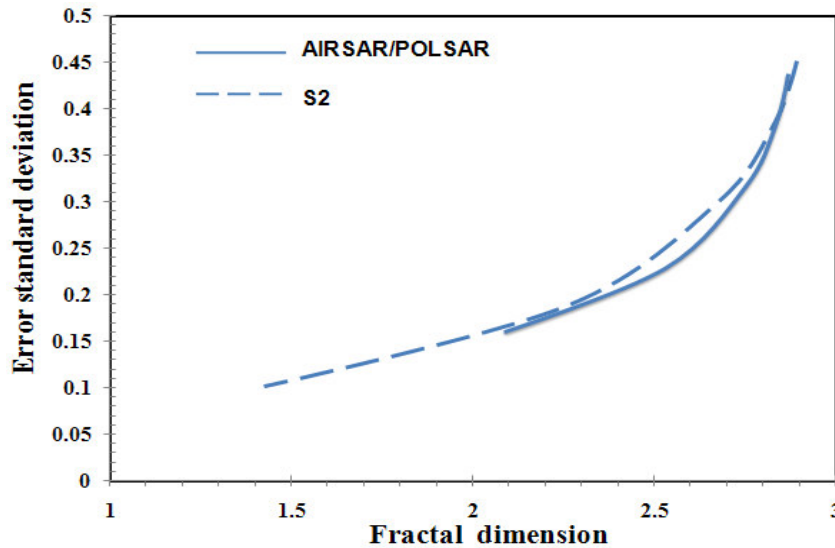


Figure 6. Accuracy assessment of fractal dimension performance.

and 3.6 in area H in AIRSAR/POLSAR and S2 mode data, respectively (Figure 4c). Furthermore, the occurrence of shear current flow could be seen in areas J, K and L, respectively in S2 mode data (Figure 4d). It was interesting to find that the fractal dimension algorithm-based probability was able to extract ship wake information in area H with a value of 3.9 (Figure 3a). This suggests that the corresponding value of fractal dimension for different categories allows a multi-fractal characterization of different features in different SAR data. These results confirmed the studies of Marghany and Mazlan (2009 a, b).

The receiver-operator characteristics (ROC) curve in Figure 5 illustrates significant differences in discrimination

between oil spill, look-alikes, and sea surface roughness pixels. In terms of ROC area, this evidence was provided by an area difference of 15% for oil spill and 45% for sea roughness and a  $p$  below 0.005, which confirms the study of Marghany et al. (2009a, b). Indeed, the fractal dimension could be viewed as a measure of the scale of the self-similarity of the object. Also, the interference was statistically similar if the scale was reduced, similar to the result of Bertacca et al. (2005). This suggests that a fractal analysis is a good method to discriminate regions of oil slick from surrounding water features.

Figure 6 shows an exponential relationship between fractal dimension and the standard deviation of the estimation error for the fractal dimension. The maximum

error standard deviation was 0.27, corresponding to the fractal dimension value of 2.9, which was found in S2 mode data. For oil spill detection, the minimum error standard deviation of 0.02 occurred in a region of fractal dimension of 1.49 in S2 mode data. For AIRSAR/POLSAR data, the maximum error standard deviation is 0.4 which corresponds to the fractal dimension value of 2.8. This means that the S2 mode performed better for detection of oil spills. In fact, the S2 mode showed a shallower incident angle than AIRSAR/POLSAR data. Wind speeds below 6 m/s are appropriate for detection of oil spills in SAR data (Solberg and Volden, 1997). Therefore, for applications that require imaging of the ocean surface, steep incidence angles are preferable as there is a greater contrast of backscatter manifested at the ocean surface.

A good discrimination between oil spill, look-alike, low wind zone and sea surface roughness exists when the error standard deviation is between 0.002 and 0.45, as produced by implementation of the fractal modified formula. The reason is that the fractal dimension is a measure of the scale of the self-similarity of the object. The low standard deviation error value of 0.002 for fractal area of 1.49 dominated by the oil spill was lower than that for the surrounding sea. This is an excellent indicator for the validation of the fractal formula modification by implementing a probability distribution function (PDF).

The fractal dimension based on the probability distribution function (PDF) improves the discrimination between oil spill, look-alikes, sea roughness and low wind zones. In fact, involving the PDF formula in the fractal dimension map directly relates the textures at different scales to the fractal dimension. Such a modification of the fractal equation reduces the problems of speckle and sea clutter and assists in the accurate classification of different textures for SAR images.

Previous studies were concerned with automatic detection of oil spills from SAR images, which is based on dark spot feature extraction and classification (Solberg and Solberg, 1996; Solberg and Volden, 1997; Benelli and Garzelli, 1999; Mohamed et al., 1999; Marghany, 2001; Marghany and Genderen, 2002; Samad and Shattri, 2002; Marghany and Mazlan, 2010d; Marghany and Mazlan, 2011). In contrast to the present study, those studies failed to detect the oil spill spreading and to discriminate between the current shear features, ship pixels, sea surface roughness and oil spill pixels by using different segmentation algorithms (Solberg and Solberg, 1996; Solberg and Volden, 1997; Mohamed et al., 1999; Samad and Shattri, 2002) or the classical fractal formula (Benelli and Garzelli, 1999; Marghany and Mazlan, 2011). Indeed, the different oil spill segmentation approaches, in terms of accuracy of classification of oil spills and features of the surrounding sea, are a challenging task; the modification of the algorithms used for automatic detection of oil spills might be required to improve the analyses (Marghany and Mazlan, 2010a).

## Conclusions

The utilization of multi SAR imagery for oil slick detection has been implemented by using a fractal dimension algorithm as an automatic tool to discriminate between an oil slick and other surface features such as slick look-alikes and variability of surface roughness. The oil spill has characteristic values of fractal dimension, which ranged between 1.49 and 2.0. The sea surface roughness has a steady value of fractal dimension which is 2.6. The interesting result is that the low wind area was characterised by the highest value of fractal dimension which is 2.48. In AIRSAR/POLSAR data, the look-alike due to natural slick has characteristic values of fractal dimension, which ranged between 1.6 and 2.0. The sea surface roughness has a steady value of fractal dimension which is 2.4. The interesting result is that the ship pixels were characterised by the highest value of fractal dimension which is 3.9. The maximum error standard deviation of 0.45 which performs with fractal dimension value of 2.9 is found in both SAR data. It can be said that the new approach of the fractal box counting dimension algorithm can be used as an automatic tool for oil spill, and look-alike detections in different sensor of SAR data.

## REFERENCES

- Aiazzi B, Alparone L, Baronti S, Garzelli A (2001). Multiresolution estimation of fractal dimension from noisy images." *SPIE-IS&T J. Elec. Imag.*, 10: 339-348.
- Benelli G, Garzelli A (1998). A multi-resolution approach to oil-spills detection in ERS-1 SAR images. *Imag. Sig. Proc. Rem. Sens.*, 4: 145-156.
- Benelli G, Garzelli A (1999). Oil-spill detection in SAR images by fractal dimension Estimation. In *Proc. of Geos. Rem. Sens. Symp. 1999, IGARSS'99, Hamburg, Germany, 28 June-2 July 1999, IEEE Geos. Rem. Sens. Soc. USA*, 2: 1123-1126.
- Bern TI, Wahl T, Anderssen T, Olsen R (1993): Oil Spill Detection Using satellite Based SAR: Experience from a Field Experiment." *Photo. Eng. Rem. Sens.*, 59: 423-428.
- Bertacca M, Berizzi F, Mese ED (2005). A FARIMA-based technique for oil slick and low-wind areas discrimination in sea SAR imagery. *IEEE Tran. Geos. Rem. Sens.*, 43: 2484-2439.
- Briggs J (1992). *Fractals: The Patterns of Chaos*. London : Thames and Hudson.
- Calaberesi G, Del Frate F, Lightenegger J, Petrocchi A, Trivero P (1999). Neural networks for the oil spill detection using ERS-SAR data. In *Proceedings of Geos. and Rem. Sens. Symp. 1999, IGARSS'99, Hamburg, Germany, 28 June-2 July 1999, IEEE Geos. Rem. Sens. Soc. USA*, 1: 215-217.
- Farahiday I, Suryono GF, Arvelyna Y (1998). Utilization of RADARSAT SAR data for oil slick detection and vessel ship monitoring application: ADRO 630 Project. *GIS and Rem. Sens. Year Book*, Academic Press, New York, BPPT 97/98.
- Fiscella B, Giancaspro A, Nirchio F, Pavese P, and Trivero P (2000). Oil spill detecting using marine SAR images. *Int. J. Rem. Sens.*, 12(18): 3561-3566.
- Falconer K (1990). *Fractal geometry*, John Wiley & Sons, New York.
- Falconer (2003). *Fractal Geometry: Mathematical Foundations and Applications*. John Wiley & Sons, Ltd.
- Fukunaga K (1990). *Introduction to statistical pattern recognition*. 2<sup>nd</sup> edition, Academic Press, New York.
- Gade M, Redondo JM (1999). *Marine pollution in european coastal*

- waters monitored by the ERS-2 SAR: a comprehensive statistical analysis. In Proc. of Geos. and Rem. Sens. Symp. 1999, IGARSS'99, Hamburg, Germany, 28 June-2 July, 1999, IEEE Geos. Rem. Sens. Soc. USA., 2: 1375-1377.
- Henschel MH, Olsen RB, Hoyt P, Vachon PW (1997). The ocean monitoring workstation: Experience Gained with RADARSAT. In CD-ROM Proc. of Geomatics in the Era of RADARSAT, Canadian Center of Remote Sensing, Canada, 25-30 May, 1997, Ottawa, Canada. Canadian Center of Remote Sensing, Ottawa.
- Maragos P, Sun FK (1993). Measuring the fractal dimension of signals: Morphological covers and iterative optimization. IEEE Trans. Sign. Proc., 41: 108-121.
- Marghany M (2001). RADARSAT automatic algorithms for detecting coastal oil spill pollution. Int. J. Appl. Earth. Observ. Geo., 3: 191-196.
- Marghany M, van Genderen J (2001). Texture algorithms for oil pollution detection and tidal current effects on oil spill spreading. Asian J. Geo., 1: 33-44.
- Marghany M (2004). RADARSAT for oil spill trajectory model. Env. Mod. Sof., 19: 473-483.
- Marghany M, Mazlan H (2005). Simulation of oil slick trajectory movements from the RADARSAT-1 SAR. Asian. J. Geo., 5: 17-27.
- Marghany M, Cracknell AP, Hashim M (2009a). Modification of fractal algorithm for oil Spill Detection from RADARSAT-1 SAR Data. Int. J. Appl. Earth Observ. Geo., 11: 96-102.
- Marghany M, Cracknell AP, Hashim M (2009b). Comparison between Radarsat-1 SAR different data modes for oil spill detection by a fractal box counting algorithm. Int. J. Dig. Ear., 2(3): 237-256.
- Marghany M, Hashim M, Cracknell AP (2007). Fractal dimension algorithm for detecting oil spills using RADARSAT-1 SAR. In Gervasi O. and Gavrilova M. (Eds.): ICCSA, Springer-Verlag Berlin Heidelberg, Part I: 1054-1062.
- Marghany M, Mazlan H (2010a). Texture entropy algorithm for automatic detection of oil spill from RADARSAT-1 SAR data. Int. J. Phys. Sci., 5(9): 1475-1480.
- Marghany MH, Arthur PC (2010b). 3-D visualizations of coastal bathymetry by utilization of airborne TOPSAR polarized data. Int. J. Dig. Ear., 3(2): 187-206.
- Marghany M, Mazlan H (2010c). Different polarised topographic synthetic aperture radar (TOPSAR) bands for shoreline change mapping. Int. J. Phys. Sci., 5(12): 1883-1889.
- Marghany M, Mazlan H (2010d). Comparison between Mahalanobis Classification and Neural Network for Oil Spill Detection Using RADARSAT-1 SAR Data. Int. J. Phys. Sci. (In Press).
- Mohamed IS, Salleh AM, Tze LC (1999). Detection of oil spills in Malaysian waters from RADARSAT Synthetic Aperture Radar data and prediction of oil spill movement. Proc. of 19<sup>th</sup> Asian Conf. on Rem. Sen., China, Hong Kong, 23- 27 November 1999, Asian Rem. Sens. Soc., Japan, 2: 980-987.
- Milan S Vachav H, Roger B (1993). Image Processing Analysis and Machine Vision. Chapman and Hall Computing, New York.
- Nirchio F, Sorgente M, Giancastro A, Biaminos W, Parisatos E, Raveras R, Trivero P (2005). Automatic detection of oil spill from SAR images. Int. J. Rem. Sen., 26: 1157-1174.
- Samad R, Mansor SB (2002). Detection of Oil spill Pollution using RADARSAT SAR Imagery. <http://www.gisdevelopment.net/aars/acrs/2002/sar/096.pdf>.
- Sarkar N, Chaudhuri B (1994). An efficient Differential Box-counting Approach to Compute fractal Dimension of Image. IEEE Tran. Sys. Man. Cyber-net., 24: 115-120.
- Solberg A, Solberg R (1996). A large-scale evaluation of features for automatic detection of oil spills in ERS SAR images. In Int. Geo. and Rem. Sens. Sym. '96, 27-31 May, 1996, Lincoln, Nebraska, IEEE Geo. Rem. Sens. Soc. USA, 3: 1484-1486.
- Solberg A, Volden E (1997). Incorporation of prior knowledge in automatic classification of oil spills in ERS SAR images. In Int. Geo. and Rem. Sens. Sym. '97, 3-8 August 1997, Singapore, IEEE Geos. Rem. Sens. Soc. USA., 1: 157-159.
- Pentland AP (1984). Fractal-based description of natural scenes. IEEE Tran. Patt. Ana. Mac. Intel., 6: 661-674, 1984.
- Redondo JM (1996). Fractal Description of density interfaces . J. Maths. Appl., 5: 210-218.
- Teivero P, Fiscella B, Gomez F, Pavese P (1998). SAR detection and characterisation of sea surface slicks. Int. J. Rem. Sen., 19: 543-548.
- Tricot C (1993). Curves and fractal dimension, Springer Verlag.
- Wornell GW, Oppenheim A (1992). Estimation of fractal signals from noisy measurements using wavelets." IEEE Tran. Sig. Proc., 40: 611-623.
- Zebker HA (1992). The TOPSAR interferometric radar topographic mapping instrument. IEEE Tran. Geo. Rem. Sens., 30: 933-940.